Coastal Dynamics 2017
Paper No. 017

WAVE TRANSFORMATION OVER THE OUANO REEF BARRIER, NEW CALEDONIA

Fabien Locatelli[1], Damien Sous[1], Vincent Rey[1], Cristele Chevalier2, Frédéric Bouchette3, Julien Touboul[1], Jean-Luc Devenon[2],

Abstract

This communication reports on a field experiments carried out on the Ouano reef barrier, New Caledonia. The analysis is based on a cross-shore network of pressure sensors deployed across the reef flat and within the lagoon. Confirming existing observations, the measurements show the strong filtering role of the reef barrier on the incoming wave energy The swell energy is dissipated and transferred toward lower frequencies, including the so-called infragravity (IG) and very low frequency (VLF) waves. During energetic event (H_s=4.2m), IG and VLF significant wave heights on the reef flat are observed to reach 1.2 and 0.7m, respectively. A variety of long waves modes are observed on the reef, combining standing and progressive-dissipative modes. In any cases, the VLF and IG waves are much more developed over and close to the reef flat than further inside the lagoon.

Key words: coral reef barrier, wave transformation, infragravity waves, very low frequency

1. Introduction

A large part of tropical shores are protected by coral reef barriers. These living systems are both priceless and threatened. They offer a nourishing shelter for a large amount of marine species. Coral reef barriers have been also shown to provide a natural and efficient protection against erosion and submersion events induced by storms or tsunamis. Unfortunately, the reef colonies and all their benefits for biological and human populations are endangered by the combined effects of the increasing anthropic pressure and the climate change (sea level rise, ocean acidification and warming).

The transformation of incoming waves over the reef barrier is of primary interest to understand the mass, energy and nutrient transfers from the open ocean to the inner lagoon which in turn affect the wealth and the renewal time of lagoon waters (Monismith, 2007). A range of processes involved in wave transformation over reef bottom has been documented by in-situ and laboratory measurements (Bonneton et al. 2007, Lowe et al. 2005, Pomeroy et al. 2012) as well as theoretical and numerical approaches (Massel and Gourlay 2000, Van Dongeren et al. 2013), including reflexion and refraction over the outside reef slope, breaking, dissipation and energy transfers toward lower and higher frequency bands.

An essential issue is to understand how the incoming swell energy is transferred to the shore or to the lagoon for fringing and barrier reef systems, respectively. Field and numerical studies demonstrated the importance of infragravity (IG) waves in reef environments (Pomeroy et al. 2012, Van Dongeren et al. 2013). In nearshore areas, these long waves are usually forced by the groupiness of incoming gravity short waves (SW), i.e. the envelope modulation of swell waves. The threshold between short and IG waves bands is generally about 0.04-0.06Hz (see Sénéchal et al. 2001 for a discussion). Under certain circumstances, a distinction can be made within the IG band itself between IG and very low frequency (VLF) bands. The usual motivation for such distinction is that in the VLF band, free surface fluctuations are more controlled by topo-bathymetric features inducing standing and/or resonating oscillations. The IG/VLF frequency boundary varies depending on the authors and the studied sites (beaches or reefs) but is typically between 0.004 (Ruessink 1998, Pomeroy et al. 2012, Van Dongeren et al. 2013) and 0.005Hz (Sénéchal et al. 2001, Gawehn et al. 2016). The lower limit for VLF (or for total IG when the IG/VLF distinction is not made) is usually taken at 0.001Hz (Aagaard and Greenwood 2008, Gawehn et al. 2016).

1 Université de Toulon, CNRS/INSU, IRD, MIO,UM110, 83051 Toulon Cedex 9, France. sous@univ-tln.fr
2 Aix-Marseille Université, Université de Toulon, CNRS/INSU, IRD, MIO, UM 110, 13288, Marseille, Cedex 09, France
3 GEOSCIENCES-Montpellier, Université de Montpellier II, Montpellier, France

In reef environments, IG waves are generated around or just before the reef top. As the outer reef slope is strong (1:20 to 1:10), the generation mechanism is generally related to the moving of the breaking point (Pomeroy et al. 2012, Baldock 2012). At the inner end of fringing reef, the shore can induce reflection of IG waves and development of standing wave motions. When the forcing period of incoming wave groups matches one of the natural seiching periods (eigenmode) of the reef flat, resonance can appear (Péquignet et al. 2009, Pomeroy et al. 2012b). Gawehn et al. (2016), which proposed a detailed classification of such processes in the case of fringing reef, indicates that resonance over reef flat is mostly observed for the longest fundamental mode around high tide.

Based on field measurement in the Ouano lagoon, New Caledonia, the present study aims to provide a new insight of wave transformation processes over a coral barrier reef. A particular attention will be paid on long waves, in order to understand how they propagate across the reef flat and are transmitted into the lagoon.

2. Experiments

2.1. Field site

The studied site is the Ouano lagoon, south-west New Caledonia. The field site is a coastal weakly anthropized narrow lagoon, nearly 30 km long, 10 km wide and 10 m deep (see Fig. 1). This reef-lagoon system is a typical "channel" lagoon with strong aspect ratio of horizontal dimensions: the lagoon is much longer than it is wide. Such configuration implies a strong effect of cross-reef fluxes induced by wave breaking on the lagoon dynamics and water renewal time. The lagoon is directly open to ocean through two reef-openings in the north-west section of the reef barrier. The southern opening is about 1 km wide and 10-20m deep while the northern is the deepest, down to -60m and 1.5 km wide. The lagoon is connected to northern and southern lagoons by two passages, one toward north and one toward south. The northern passage is about 5m deep while the south passage is 10-15 m deep. Note that this latter is close to a further south reef-opening. At high tide, the coral reef barrier is fully submerged, whereas at low tide it can be partly emerged depending on tide and wave conditions as well as large-scale sea level fluctuations. For further description of the Ouano reef-lagoon system, the reader should refer to Chevalier et al., 2015.

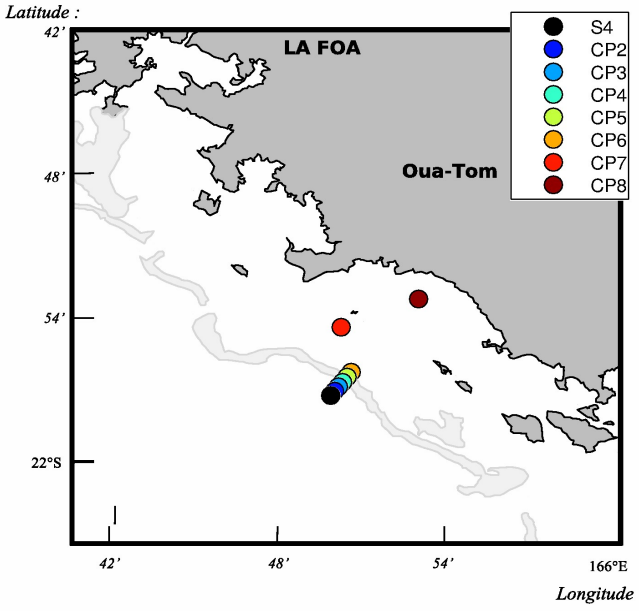

Figure 1. The Ouano reef-lagoon system, New Caledonia. Light grey zones indicate most of the reef colonies. Positions of the reef barrier sensors (S4, CP2-CP6) are distorted, precise values are given in Fig. 2.

2.2. Instrumentation and methods

The field measurements presented here are part of a large hydro-biogeochemical field campaign (OLZO and CROSS-REEF projects) conducted from April to August, 2016. The instrumentation used for the present analysis is dedicated to the study of cross-reef wave transformation and propagation within the lagoon. Incoming wave conditions are provided by a S4 electro-current meter (8 m deep) on the reef foreshore on 20 min bursts recorded each 3h. Due to the failure of the embedded pressure sensor, free surface fluctuations at S4 are deduced from the velocity measurements using linear wave theory. Seven autonomous pressure sensors have been deployed from the reef top to the inner lagoon. The reef flat sensors CP2 to CP5 are OSSI Wave Gauge® sensors recording bottom pressure at 5 Hz. The lagoon pressure sensors are RBR Duo® at 2Hz. Positioning of the sensors array is given in Fig. 2.

Energy spectra presented in Fig. 3 are computed continuously over 40min burst for each pressure sensor (see Sec. 3.1 for discussion). Figure 3 displays the average spectra over the April 25 to July 31 time period. The average spectrum of the wave field envelope measured by S4 is computed each 3h over 20min bursts using Hilbert transform.

Bathymetric data results from in-situ surveys performed during the campaign and combined with the ZONECO atlas. It should be noted the acquisition of reliable bathymetric data in reef area remains quite challenging, in particular in the zones exposed to waves. The bathymetry of the inner reef coral colony has not been properly documented and is given as indicative information in Fig. 2 from sparse data survey and visual observations.

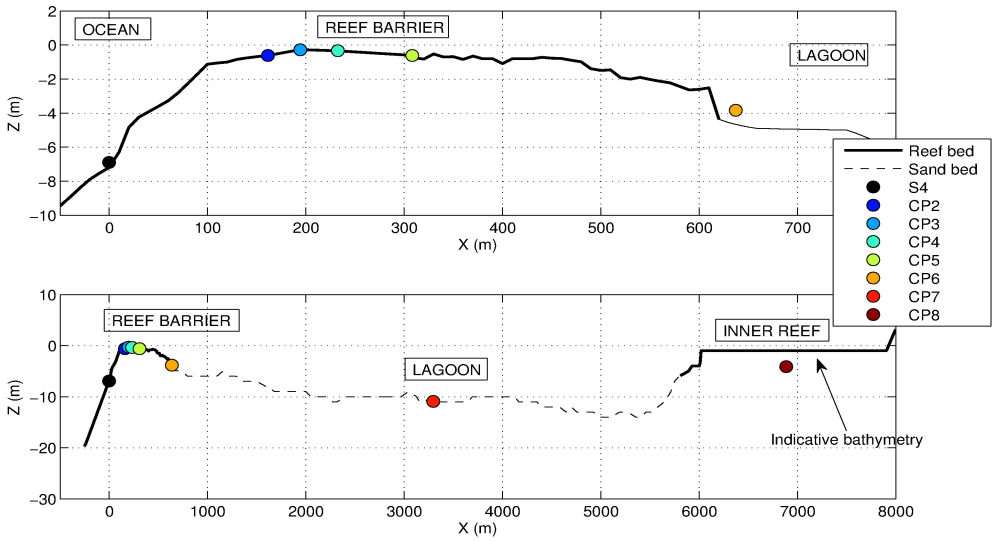

Figure 2. Experimental Setup along the studied cross-shore transect (upper plot is a zoom on the reef barrier area). Inner reef bathymetry is indicative (for X>6000m) as no survey data is available. Note that CP7 sensor is not aligned with other sensors (see Fig. 1)

3. **Results**

3.1. Theoretical seiching modes

Fringing reefs have been observed to develop a specific dynamics for long waves, partly controlled by strong reflection process at the shore inducing standing or resonant VLF modes attached to the reef flat. Barrier reef systems are not that constrained due to the presence of a fluid rather than a rigid boundary at the inner limit of the reef flat. They however show strong topo-bathymetric gradients able to potentially induce partial reflection of surface waves. It is well-know that wave reflection in closed or semi-open

basins leads to the development of standing waves, the so-called seiches. In order to estimate the seiching modes for our reef-lagoon system, we use the analytical work of Wilson (1972), restated by Rabinovich (2009).

Two types of standing oscillations can *a priori* be expected. First, the lagoon can be considered as a basin either closed or semi-open at the reef boundary. In the former case, the expected fundamental seiching wave has a node near the basin center and two anti-nodes at the lagoon boundaries. The oscillation period depend on the water depth and the exact bathymetric profile, but assuming a 12m deep 6000m long flat basin, the fundamental frequency is f_0=9.4.10^{-4} Hz. Higher nth harmonics are at $n.f_0$. If the basin is considered semi-open, seiching frequencies are $((2n+1)/2).f_0$. The fundamental mode ($n=0$) shows a node at the reef barrier and an anti-node at the inner reef.

Second, the reef flat itself shows a strong bathymetric gradients at its boundaries, in particular a nearly vertical step at its inner end. This induces discontinuities in the wave celerity which can possibly induce partial reflection of surface wave. The reef standing wave pattern would thus consists in a node/anti-node at the barrier outer/inner boundary. Possible seiching oscillations attached to the reef barrier would naturally be more dependent on depth, because relative depth fluctuations are much more important on the reef than in the lagoon. The fundamental mode for the reef barrier seiche is at f_0=1.4.10^{-3} Hz.

Each of these fundamental modes are in the usual VLF range. The selected 40 min time window for spectral analysis is long enough to resolve the expected VLF scales (Gawehn et al. 2016). It is emphasized that the theoretical values, which are used as a guide for the data analysis, must be considered keeping in mind the limitations of the idealized case. First, the predictions are provided for flat basin which do not account for bathymetry variations which can strongly affect long waves structure (Michallet et al. 2007) neither for the effect of bed friction. Second, this purely cross-reef longitudinal analysis discard any wave pattern developing in the long axis of the lagoon. Finally, one notes the possible overlapping between seiche harmonics in the lagoon or over the reef which increases the complexity of the analysis.

3.2. Wave classification

The first step of the data processing is the characterization of the free surface waves observed along the instrumented cross-shore transect.

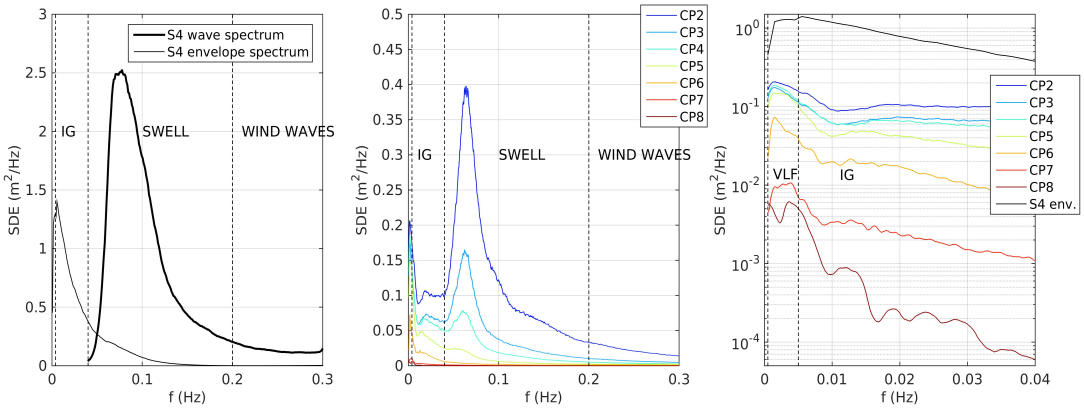

Figure 3. Average wave spectra over the whole acquisition period. Right: SW and envelope spectra deduced from velocity measurements over the outer reef slope (S4, 20min spectra every 3h). Center and right: full spectra for pressure sensors (CP2-CP8, continuous 1h measurements). The right plot is a zoom in the low frequency band.

Figure 3 shows that in the short-wave (SW) or so-called "gravity" band (0.04<f<0.3 Hz) which combines swell and wind waves, the average spectrum depicts a swell-dominated environment. Peak periods between 14 and 22s correspond to long south pacific swells reaching the studied reef with a nearly normal incidence. Shorter waves with peak periods around 7s generally correspond to more south-easterly waves. At higher frequencies, the free surface oscillations are mostly wind waves locally generated by trade winds modulated by thermal winds but, further over the reef flat, they can also result from the energy transfer to higher harmonics already observed here (Chevalier et al. 2015) or in other sites (Masselink 1998). The averaged spectrum of SW envelope over the reef foreshore (thin line in Fig. 3, left) shows that 3-months

averaged SW modulations increase with decreasing frequency (as denoted for instance by Van Dongeren et al. (2013) and reach a peak around 0.0055Hz, i.e. just above the selected IG-VLF limit. Envelope energy remains quite high in the upper VLF band and falls quickly below 0.0015Hz (Fig.3, right plot).

Fig. 3 (right plot) shows a zoom on low frequency for the 3-months averaged spectra. The SW-IG limit is here taken at 0.04Hz as suggested by Van Dongeren et al. (2013) and well adapted to our long swell dominated environment. For the IG-VLF limit is less straightforward, the 0.005Hz value proposed by Gawehn et al. for fringing reef is depicted in Fig. 3 as a guide. For the reef flat sensors (CP2-CP6), a peak is observed is the VLF band around 0.0015Hz. Below this value, VLF energy on the reef barrier quickly decreases, which can be directly related to the drop of SW envelope energy. However, the 0.0015Hz value also appears in good agreement with the theoretical fundamental reef flat seiching oscillation but further analysis is required to better identify the possible presence of standing wave motions. The energy decreases with increasing frequency and increases again in the IG band after a trough around 0.01Hz. The overall energy decreases significantly when moving into the lagoon and this shoreward attenuation increases with frequency. The inner lagoon is mainly controlled by VLF motions. Specific spectral modulations are observed for CP7 and CP8 sensors. They both show a common peak around 0.0035Hz but CP7 (mid lagoon) also shows the 0.0015Hz peak than the reef sensors whereas CP8 (inner reef) is characterized by a clear energy minimum around 0.0023Hz and is maximal for the lowest part of the VLF band around 0.0009 Hz. This latter may fairly correspond to the anti-node of the fundamental seiching mode of the lagoon considered as a closed basin.

3.2. Wave climate

The analysis of surface waves climate in the reef-lagoon system is based here on the data recovered during the month of May, 2016, during which various conditions of waves, tides and sea level have been encountered. Time series for significant wave height for VLF, IG and SW are plotted in Fig. 4 together with 1h and 24h averaged mean sea level over the reef flat (CP5 sensor, top plot).

Let us first focus on the SW transformation depicted in Fig. 4. The results confirm the well-know strong filtering role played by the reef on the incoming swell energy (Hardy and Young 1996, Hearn 1999). The SW amplitude decreases as propagating over the reef barrier due to the combined effects of breaking, frictional dissipation and harmonic transfers. Each of these processes are governed by the water depth over the reef. The reef barrier acts thus as a tide-controlled filter of SW energy: the lower the depth, the stronger the attenuation. Wave breaking occurs in most cases between S4 and CP2, leading to a strong decrease of SW energy. It is only during very calm wave and high tide conditions that wave breaking occurs higher on the reef flat, as already observed by Chevalier et al. 2015.

A series of observations on IG and VLF surface waves dynamics can be performed from Fig. 4. One notes first that overall VLF, IG and SW significant heights are well correlated: strong IG/VLF periods correspond to strong incoming waves. During the very strong swell event on May, 22 (Hs=6m, Tp=16s), the IG and VLF amplitudes reach 1.2 and 0.7m, respectively. An example of free surface elevation recording at CP5 on May, 22, is depicted in Fig. 5. One notes the combination of VLF, IG and SW fluctuations with periods of the order of 10 min, 1-2min and 15s, respectively. The wave pattern is here quite different than the VLF waves measured by Gawehn et al. 2016 on the Roi-Namur Island fringing reef. VLF waves are here more regular and do not show the bore waveform observed by Gawehn et al. These long oscillations rather appear to act as carrier waves for the higher frequency wave field resulting from the superposition of IG and SW.

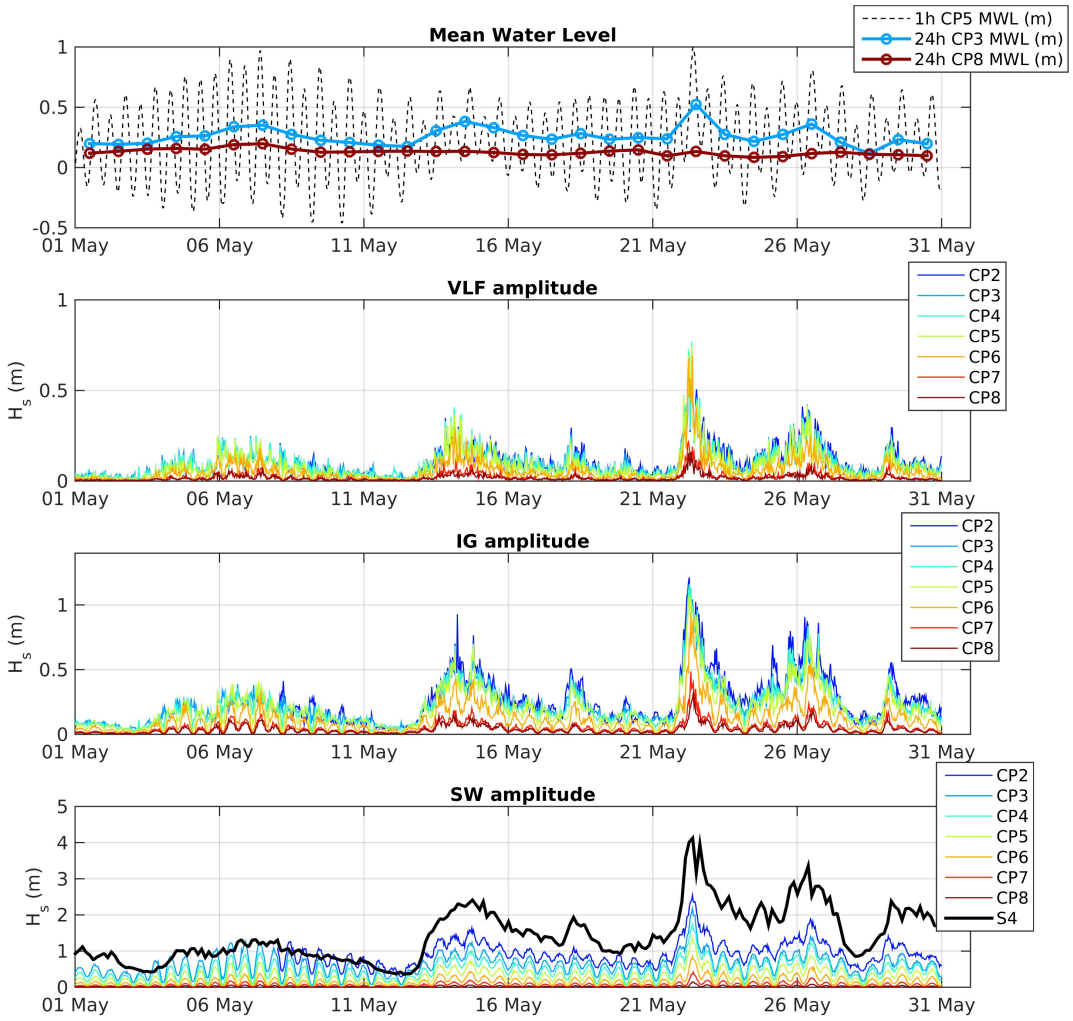

Figure 4. Time series of VLF, IG and SW significant wave amplitude continuously computed over 1h bursts. Incoming swell significant wave height at the reef foreshore (S4) is computed over 20min bursts each 3h. The top plot depicts the Mean Water Level (1h averaged at CP5) and the 24h averaged levels measured at CP3 and CP8.

Figure 4 shows that, when the incoming wave energy is significant (typically *Hs*>*2*m), the IG waves energy generally decreases along the reef transect toward the inner lagoon. This process is modulated by the tidal elevation with more energy propagating along the barrier as the tide level rises. This trend is less straightforward when the swell is small and/or the tidal range is large. For the higher tidal ranges (see e.g. the low tides of May 8-11), the reef top is at least partly emerged at low tide. A very strong dissipation of IG waves is observed on the offshore part of the reef flat and nearly no waves are observed after CP3. At high tide, CP2-CP6 sensors show very close IG amplitude indicating a small IG waves dissipation when water depth is high and incoming swell rather moderate. The VLF dynamics is also strongly dependent on the incoming swell amplitude but the effect of tide is quite lower than for IG. The general trend is a general decay along the instrumented transect. However, for the stronger swells (May 14-15 or 22) the VLF energy is nearly steady across the reef barrier (CP2-CP6 sensors).

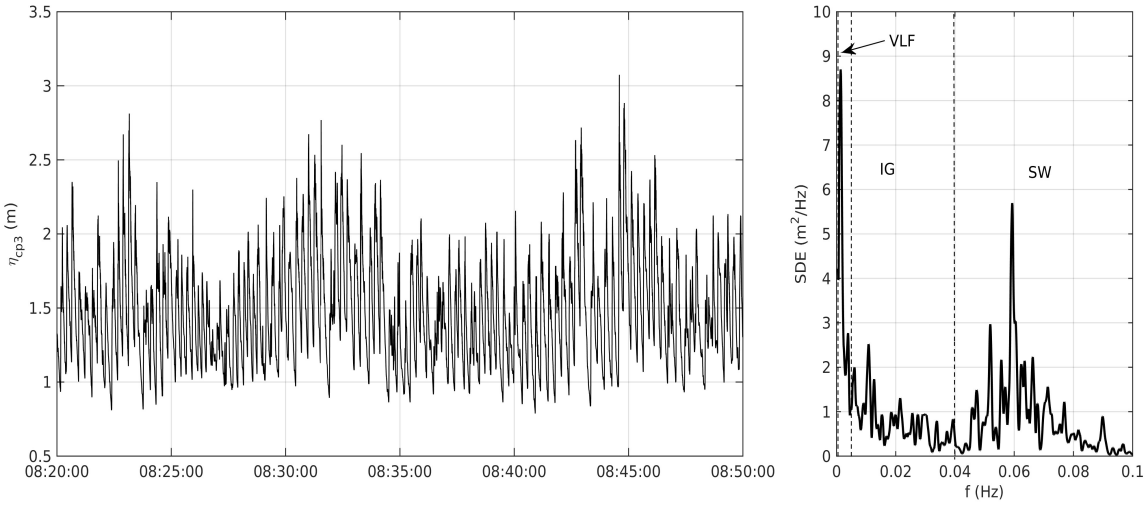

Figure 5. May, 22 swell event, CP3 reef top measurements. Left: free surface elevation from pressure measurements. Right: spectral density of energy.

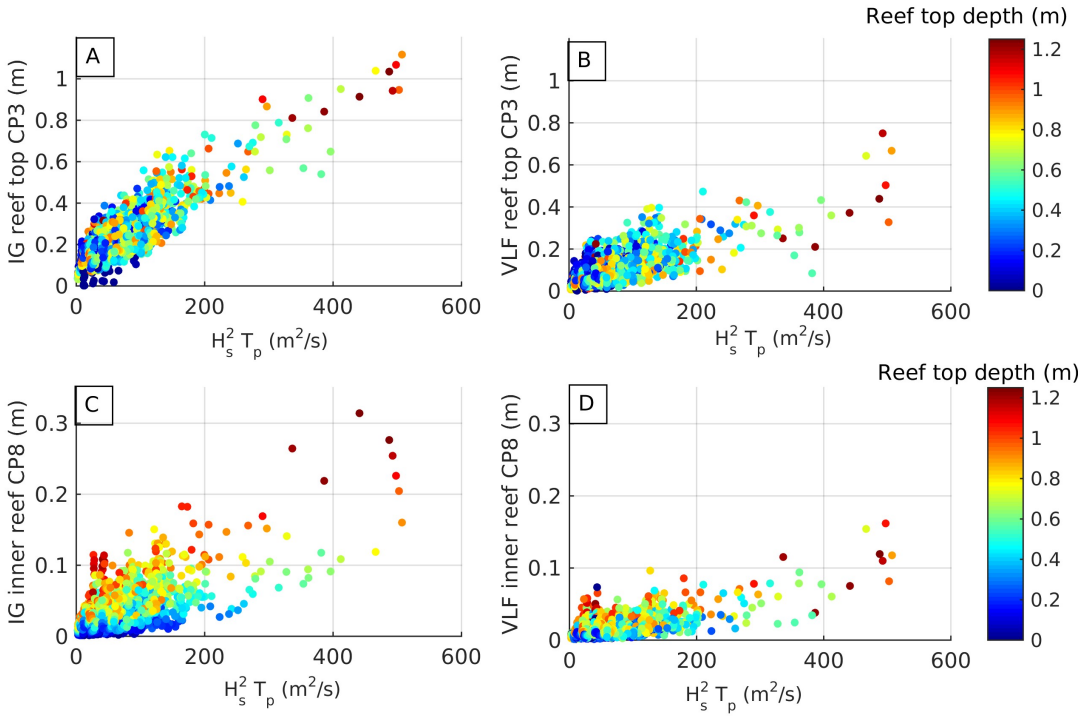

Figure 6. IG and VLF significant wave heights vs SW incoming energy flux for reef top CP3 (A,B) and inner reef CP8 (C,D) sensors for the month of May, 2016. The color levels depict the water depth above the reef top. Note the difference in y-axis for A,B and C,D plots.

The dependence of IG waves produced on the reef top on the incoming wave field is best predicted by the parameter $H_s^2 T_p$ measured at the reef foreshore (see Fig. 6, A), similarly to the data obtained by Inch et al. (2017) on dissipative sandy beach. The VLF amplitude over the reef top (Fig. 6, B) show a lower dependence on incoming energy, with more dispersion. The VLF/IG ratio over the reef top is around one

third. The same analysis is performed for the inner reef sensor (CP8). The general trend is similar, i.e. more incoming energy produces more IG/VLF within the lagoon, but the role of water depth over the reef top is much more important. This is particularly visible for IG waves at CP8: the higher the free surface over the reef, the stronger the IG wave motions inside the lagoon. This confirms the strong dissipation of IG waves on the reef barrier, modulated by the water depth. As water level over the reef decreases, bottom friction over the reef increases the damping of IG energy produced in the surf zone and further reduces the IG wave propagating within the lagoon. The same tendency is observed for VLF at CP8, although with a larger spread. One notes also that, in a general manner, long waves are strongly attenuated in the lagoon itself. This is particularly true for VLF, for which a minimal threshold of energy flux is necessary to induce clear fluctuations whereas VLF waves over the reef top are observed to rise as soon as the incoming SW energy increases.

An additional observation can be performed on the reef top MWL (CP3) depicted in Fig. 4: the strong wave setup on the reef top, up to 40cm during swell events, which will be involved in the development of significant pressure gradients and currents across the reef barrier (Hearn 1999, Bonneton et al. 2007).

3.3. Wave transformation

Figure 7 depicts the IG and VLF transformations along the studied transect. Let us first focus on the IG waves evolution. Between CP2 and CP3, the IG dynamics depends on both incoming SW amplitude and tide elevation. When incoming swell is strong (typically greater than 2.5m at the foreshore), the breaking zone is on the outer reef slope. Consequently most of IG waves are produced well upstream the reef top and a significant dissipation is already observed between CP2 and CP3. This process is dependent on tide, and the dissipation decreases as water level increases. However, in any case of strong swell, the ratio between significant IG heights at CP3 and CP2 remains less than 1. For moderate and small incoming SW, the ratio can reach values up to 1.9. This indicates that, for such moderate wave events, production of IG waves occurs between CP2 and CP3. The tendency is again controlled by the tide: when the still water level lowers, the breaking zone and IG production shift offshore and dissipation process can dominate. Further onshore on the reef flat (CP3 to CP4 and CP4 to CP5), the transformation, which should mainly result from the competition between production and dissipation, is now fully controlled by tidal fluctuations. At low tide, the dissipation is very strong and IG waves amplitude are observed to decrease of more than 90% in 120m between CP3 and CP5). Between mid and high tide, the tidal effect on wave transformation is less intense than between low and high tide and amplification of IG waves can be observed. This non-linear response to tide indicates that for the lower levels, IG are only produced offshore the reef top and the IG dynamics is only controlled by dissipation, while for higher mean water levels, IG production is still active over the reef flat. Between CP5 and CP6, one notes a nearly unimodal dependence of IG transformation on the tide elevation and a systematic damping. This trend confirms the previous observations of the progressive transition from production to dissipation regimes for IG waves across the reef flat. Within the lagoon, i.e. between CP6 and CP8, the tide effect is nearly invisible but a strong damping (about 70%) is observed. Such a damping can be attributed to bottom friction processes, both over the sand bottom and the inner reef of the Ouano lagoon.

For VLF waves, the general trend is generally the same, i.e. an overall decrease from the reef top to the inner reef. The tidal effect is less marked. Between CP2 and CP3 (outer reef flat), the influence of swell previously noticed for IG waves is still valid: for strong swells, the VLF amplitude generally decreases while for smaller swells, strong amplification can be observed. This trend can again be related to the offshore shifting of breaking zone and VLF production during strong swell conditions. However, more importantly, a striking observation for each reef flat sensors is that VLF are amplified in a number of cases. This naturally raises the question of the part of standing or even resonant motions in the VLF band. The question can be also triggered for IG waves, but the first, and consistent, analysis performed herein before only assumes purely propagating waves.

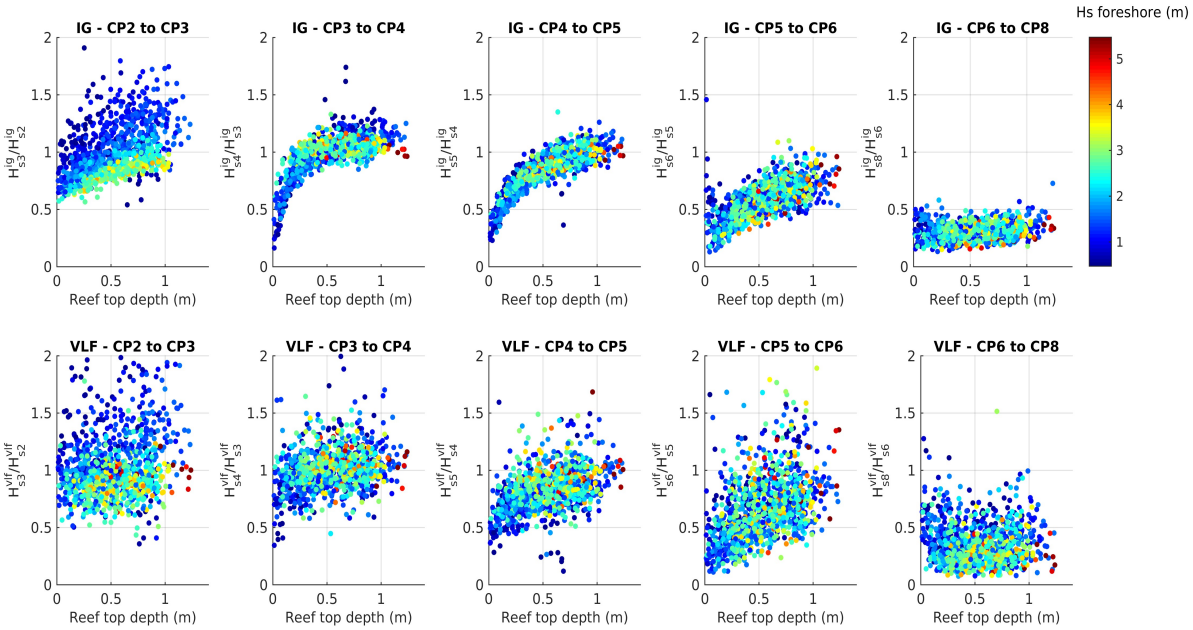

Figure 7. Long waves transformation along the cross-shore transect. Top and bottom plots are IG and VLF, respectively. Each plot is a ratio of significant wave heights between two consecutive sensors vs the water depth over the reef top. Color levels depict the SW significant height at the foreshore sensor (S4).

3.4. Standing vs progressive wave patterns

To better understand the long wave dynamics, and in particular to discriminate the possible presence of standing wave motions in our system, we use part of the approach proposed by Pomeroy et al. (2012b) and Gawehn et al. (2016). The analysis presented in Fig. 8 is first based on the calculation of the magnitude squared coherence between the signal recorded at two distinct sensors:

$$C_{xy}(f) = \frac{\left|G_{xy}(f)\right|^2}{G_{xx}(f)\,G_{yy}(f)}$$

where $G_{xy}(f)$ is the cross-spectral density between x and y, and $G_{xx}(f)$ and $G_{yy}(f)$ the autospectral density of x and y, respectively. When the coherence is close to one, the signals are in direct relationship. The coherence is computed and averaged over the month of May (Fig. 8, A). Then two specific events (May 15, 16:00 and May 22, 6:00) are selected, with 40 min bursts taken at the same depth over the reef top (0.7m) in two different wave conditions: strong swell (Fig. 8, B) and very strong swell (Fig. 8, C).

As emphasized by Pomeroy et al. (2012b), the coherence can not itself reveal the presence of a standing wave because "... any wave form that propagates across a basin and maintains a (reasonable) consistent form will have a high coherence.". A second indicator is thus used to better understand the relationship between long wave pattern at two different measurement points: the phase lag between the two signals (Fig. 8, D and E). A special attention is paid on the phase lags for the CP2-CP3, CP3-CP4, CP2-CP6 and CP6-CP8. If standing wave motions develop on the reef flat or within the lagoon following the theoretical approach (Sec. 3.1), neighboring sensors CP2-3-4 should be nearly in phase (Lag=0) while CP2-CP6 or CP6-CP8 should be out-of-phase (Lag around $\pm\pi$) with strong coherence in each case. Note that the reef flat sensors are not strictly at the limits of the expected seiching domains, so difference to these theoretical values are expected.

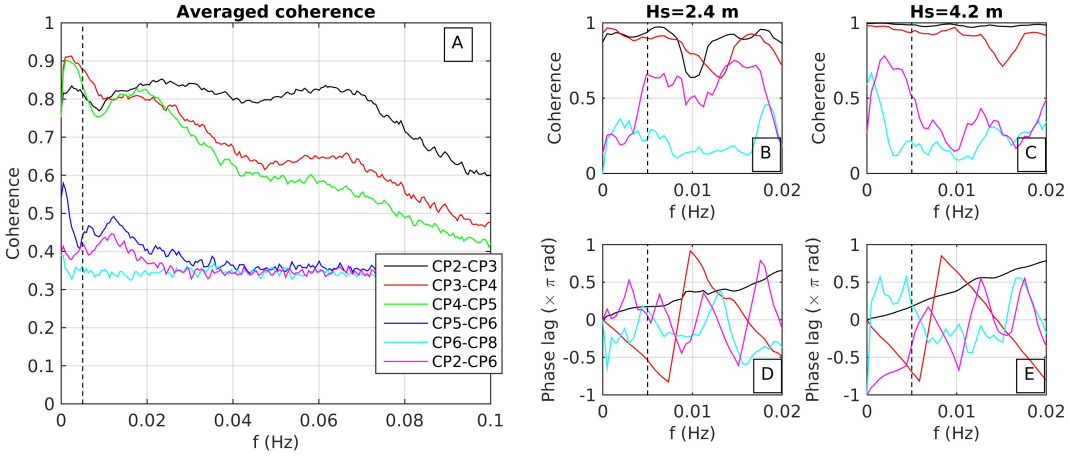

Figure 8. A: Averaged magnitude-squared coherence for neighboring sensors over the month of May. B and C: Magnitude squared coherence for 40 min bursts on May 15, 16:00 and May, 22 6:00. D and E: Phase lag for 40 min bursts on May 15, 16:00 and May, 22 6:00. For both events, the mean water depth above the reef top is 0.7m. Vertical dashed line on each plot correspond to th IG-VLF threshold.

The month-averaged coherence for the reef flat sensors (CP2 to CP5) in Fig. 8 shows that, as expected, the coherence generally increases as the frequency decreases. For the higher part of the IG band ($0.03<f<0.05$ Hz) and further for gravity waves, strong wave transformations occur after the reef top as observed on the smaller coherences for CP3-CP4 and CP4-CP5 sensor pairs. In the lower part of the IG band ($0.005<f<0.03$Hz), the coherence remains high all across the reef flat. It still increases when entering the VLF band for CP3-CP4 and CP4-CP5 pairs but is a bit lower on the outer reef flat slope between CP2 and CP3. The averaged coherence drastically decrease further onshore. Between CP5 and CP6, a moderate coherence is observed mainly for low VLF, while between CP6 and CP8 such peak is hardly visible.

The analysis of the two selected events reveals the importance of the swell energy. For the 2.4m swell depicted in Fig. 8 B and D, strong coherence is observed for CP2-3-4 in both IG and VLF bands. The CP2-CP6 coherence strongly falls when entering the VLF band. This indicates that, even if VLF energy is transmitted toward the lagoon, the wave forms are altered. The phase lags for the same event (Fig. 8, D) show ramps for the reef flat sensor. This linear dependency on frequency indicates the presence of progressive waves in both VLF and IG bands. In the inner lagoon (CP6-CP8), no clear cross-shore wave propagation can be identified. The pattern is drastically different for the 5.2m swell event of May, 22. Coherence for sensors CP2-3-4 is still very strong (even increased). In the VLF band, significant coherence peaks are observed at 0.002-0.003Hz and 0.0005Hz for CP2-6 and CP6-8 sensors pairs. Phase lags show the similar frequency ramp patterns for the reef flat sensors but the frequencies associated to coherence peaks in the VLF reveal: (i) a $\pi/4$ phase lag between CP6 and CP8 around 0.0005Hz and, (ii), a lag around $3\pi/4$ between CP2 and CP6 in the 0.0014-0.0019Hz range. The former fairly corresponds to the fundamental seiching mode of the lagoon considered here as *a semi-open basin* while the latter is in the range of the fundamental mode expected for seiching oscillations on the reef flat domain due to partial wave reflection at the reef barrier boundary. Further analysis is now required to better discriminate such bimodal standing wave pattern and, in particular, to understand their response on incoming wave conditions and tidal fluctuations.

4. Conclusion

The present study is a part of a large scale experiments performed on the Ouano barrier reef lagoon system, New Caledonia. A long term field campaign has been carried out to monitor the wave transformation from the reef foreshore to the inner lagoon. The measurements, based on a cross-shore network of pressure sensors, revealed the presence of strong long wave dynamics over the reef flat divided into the so-called infragravity (IG) and very low frequency (VLF) waves. The IG/VLF energy produced on the reef is

directly related to the incoming swell energy flux. The filtering role played by the reef barrier, through wave breaking and frictional processes, is strongly depend on the water depth: the lower the tide, the stronger the dissipation.

Dedicated analysis has been carried out to identify the possible presence of standing long waves in our system. It appears that, at least for the most energetic event recorded (H_s=4.2m, T_p=15s), two patterns of seiching modes can be observed. The first is associated to the fundamental oscillation of the lagoon, considered as a semi-open basin, in its transverse direction. The second is attached to the reef barrier itself, possibly induced by partial reflection of the long waves by the bathymetric step at the reef/lagoon boundary. Further research work has to be engaged to confirm these observation and better understand the conditions for VLF/IG waves development and attenuation. In addition, a particular attention will be paid on the role of cross-reef currents, which are strong and vertically sheared, on the wave dynamics.

Acknowledgements

This study was sponsored by the EC2CO OLZO program (CNRS INSU), the OLZO and CROSS-REEF Action Sud (MIO IRD) and the ANR project MORHOC'H (ANR-13-ASTR-0007). The Noumea IRD center and the GLADYS group supported the experimentation. We are grateful to all the contributors involved in this experiment. The authors are particularly indebted to David Varillon, Eric Folcher and Bertrand Bourgeois whose efforts were essential to the deployment and Pascal Douillet for providing free access to bathymetric data.

References

Aagaard, T. and Greenwood B., 2008. Infragravity wave contribution to the surf zone sediment transport – the role of advection, *Marine Geology,* 251: 1-14.

Baldock, T. E., 2012. Dissipation of incident forced long waves in the surf zone – Implications for the concept of "bound"wave release at short wave breaking, *Coastal Engineering,* 60: 276-285.

Bonneton, P., Lefebvre, J. P., Bretel, P., Ouillon, S., and Douillet, P., 2007. Tidal modulation of wave-setup and wave-induced currents on the Aboré coral reef, New Caledonia, *J. Coast. Res*, 50:762-766.

Chevalier, C., Sous, D., Devenon, J. L., Pagano, M., Rougier, G., and Blanchot, J., 2015. Impact of cross-reef water fluxes on lagoon dynamics: a simple parameterization for coral lagoon circulation model, with application to the Ouano Lagoon, New Caledonia, *Ocean Dynamics*, *65*(11): 1509-1534.

Gawehn M., van Dongeren A., van Rooijen A., Storlazzi C. D., Cheriton, O. M. and Reniers, A., 2016. Identification and classification of very low frequency waves on a coral reef flat, *Journal of Geophysical Research: Oceans,* 121.

Hardy, T. A. and Young, I. R., 1996. Field study of wave attenuation on an offshore coral reef, *Journal of Geophysical Research:Oceans,* 101: 14311–14326.

Hearn, C.J., 1999. Wave-breaking hydrodynamics within coral reef systems and the effect of changing relative sea level*, Journal of Geophysical Research,* 104: 30007-30019.

Inch, K., Davidson, M., Masselink, G. and Russell, P., 2017. Observations of nearshore infragravity wave dynamics under high energy swell and wind-wave conditions. *Continental Shelf Research*, 138, pp.19-31.

Lowe, R. J., Falter, J. L., Bandet, M. D., Pawlak, G., Atkinson, M. J., Monismith, S. G., and Koseff, J. R.,2005. Spectral wave dissipation over a barrier reef, *Journal of Geophysical Research: Oceans*, 110: C4.

Massel, S. R., and Gourlay, M. R., 2000. On the modelling of wave breaking and set-up on coral reefs, *Coastal engineering*, *39:* 1-27.

Masselink, G., 1998. Field investigation of wave propagation over a bar and the consequent generation of secondary waves, *Coastal Engineering,*33: 1-9.

Michallet, H., Grasso, F., and Barthelemy, E., 2007. Long waves and beach profile evolutions, *Journal of Coastal Research,* 50, 221.

Monismith, S. G., 2007. Hydrodynamics of coral reefs, *Annu. Rev. Fluid Mech.,* 39: 37-55.

Péquignet, A. C. N., J. M. Becker, M. A. Merrifield, and J. Aucan, 2009. Forcing of resonant modes on a fringing reef during tropical storm Man-Yi, *Geophys. Res. Lett.,* 36, 20–23

Pomeroy, A., Lowe, R., Symonds, G., Van Dongeren, A., and Moore, C., 2012. The dynamics of infragravity wave transformation over a fringing reef, *Journal of Geophysical Research: Oceans*, 117:C11.

Pomeroy, A. W. M., A. van Dongeren, R. J. Lowe, J. S. M. van Thiel de Vries, and J. A. Roelvink, 2012b. Low frequency wave resonance in fringing reef environments, *Proc. 33rd International Conference on Coastal Engineering, Santander, Spain*, 1(33), pp. 1–10

Rabinovich, A. B. 2009. Seiches and harbour oscillations, *Handbook of Coastal and Ocean Engineering, World Scientific, Singapore,* 193–236,.

Ruessink, B.G., 1998. Bound and free infragravity waves in the nearshore zone under breaking and nonbreaking conditions, *Journal of Geophysical Reaseach,* 103:12795-12805.

Sénéchal, N., Dupuis. H., Bonneton, P., Howa, H. and Pedredos, R., 2001. Observation of irregular wave transformations in the surf over a gently sloping sandy beach on the French Atlantic coastline, *Oceanologica Acta.* 24: 6.

Thornton, E. B., and Guza, R. T., 1983. Transformation of wave height distribution, *Journal of Geophysical Research: Oceans*, 88: 5925-5938.

Van Dongeren, A., Lowe, R., Pomeroy, A., Trang, D. M., Roelvink, D., Symonds, G., and Ranasinghe, R., 2013. Numerical modeling of low-frequency wave dynamics over a fringing coral reef, *Coastal Engineering*, 73:178-190.

Wilson, B.W., 1972. Seiches, *Advances in hydroscience*. 8: 1-94.